Defect reconstruction in waveguides using resonant frequencies

Angèle Niclas

Collaboration with
Éric Bonnetier, Claire Prada, Laurent Seppecher, Grégory Vial

Context

Goal: Non destructive monitoring of industrial structures called waveguides modeling pipes, optic fibers, metal plates, boat hulls, aircraft parts, train tracks...

Figure: Practitioners monitoring of a pipeline.

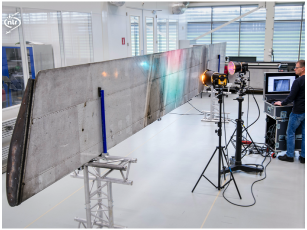

Figure: Practitioners monitoring of a aircraft part.

Context

Goal: Non destructive monitoring of industrial structures called waveguides modeling pipes, optic fibers, metal plates, boat hulls, aircraft parts, train tracks...

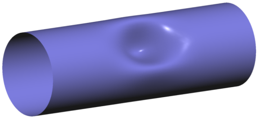

Figure: Width defect in a 3D acoustic pipe.

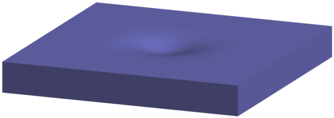

Figure: Width defect in a 3D elastic plate.

Context

Goal: Non destructive monitoring of industrial structures called waveguides modeling pipes, optic fibers, metal plates, boat hulls, aircraft parts, train tracks...

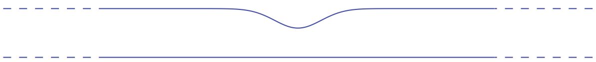

Figure: Width defect in a 2D acoustic pipe or elastic plate.

State of the art

Usual experimental setup:

State of the art

Usual experimental setup:

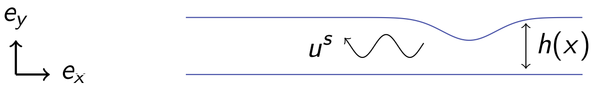

State of the art

Usual experimental setup:

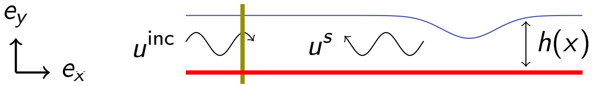

Measurement of $u^{\text{tot}} = u^{\text{inc}} + u^s$ on a surface or on a section.

State of the art

Usual experimental setup:

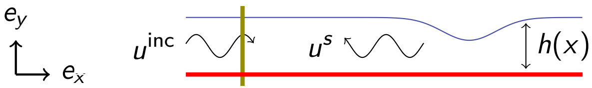

Measurement of $u^{\text{tot}} = u^{\text{inc}} + u^s$ on a surface or on a section.

- Fixed frequency, different incident waves: Linear sampling method [Colton, Kirsch 96] [Bourgeois, Lunéville 08], Far-field asymptotic developments [Dediu, McLaughlin 06]...
- Multi-frequency, one incident wave: MUSIC algorithm [Bao, Triki 13], Far-field asymptotic developments [Borcea, Nguyen 16]...

State of the art

Usual experimental setup:

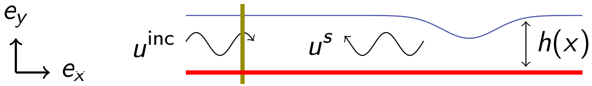

Measurement of $u^{\text{tot}} = u^{\text{inc}} + u^s$ on a surface or on a section.

- Fixed frequency, different incident waves: Linear sampling method [Colton, Kirsch 96] [Bourgeois, Lunéville 08], Far-field asymptotic developments [Dediu, McLaughlin 06]...
- Multi-frequency, one incident wave: MUSIC algorithm [Bao, Triki 13], Far-field asymptotic developments [Borcea, Nguyen 16]...

State of the art

Usual experimental setup:

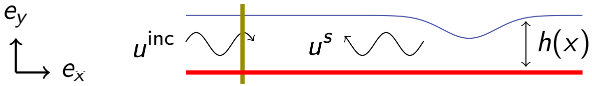

Measurement of $u^{\text{tot}} = u^{\text{inc}} + u^s$ on a surface or on a section.

- Fixed frequency, different incident waves: Linear sampling method [Colton, Kirsch 96] [Bourgeois, Lunéville 08], Far-field asymptotic developments [Dediu, McLaughlin 06]...
- Multi-frequency, one incident wave: MUSIC algorithm [Bao, Triki 13], Far-field asymptotic developments [Borcea, Nguyen 16]...

Commun point: all these methods avoid some frequencies, called resonant frequencies, of the waveguide.

Contents

Outline

1. Perfect waveguides and resonances
   - Modal decomposition
   - Resonant frequencies

2. Perturbed waveguide - acoustic case
   - Approximation of the forward problem
   - Inverse problem and numerical reconstructions

3. Tools to reconstruct defects in elastic waveguides
   - Modal decomposition
   - Adaptation of the inversion method

4. Ongoing projects

Wave propagation in perfect waveguides

Let $\Omega = \mathbb{R} \times (0, h)$ be a perfect waveguide where $h > 0$ denote the width of the waveguide.

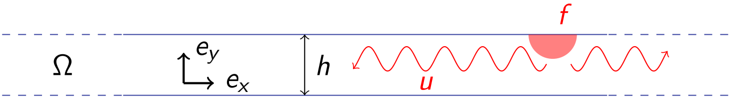

Wave propagation in perfect waveguides

Let $\Omega = \mathbb{R} \times (0, h)$ be a perfect waveguide where $h > 0$ denote the width of the waveguide.

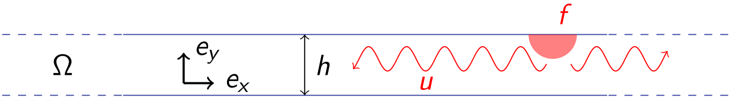

A wavefield u propagates in Ω at frequency $k > 0$ according to the Helmholtz equation:

$$\begin{cases} \Delta u + k^2 u = -f & \text{in } \Omega, \\ \partial_\nu u = 0 & \text{on } \partial\Omega, \\ u \text{ is outgoing.} & \end{cases} \tag{1}$$

Modal decomposition

We define each mode $n \in \mathbb{N}$ of the waveguide by

$$\varphi_n = \begin{cases} \dfrac{1}{\sqrt{h}} & \text{if } n = 0, \\ y \mapsto \dfrac{\sqrt{2}}{\sqrt{h}} \cos\left(\dfrac{n\pi y}{h}\right) & \text{else.} \end{cases} \tag{2}$$

Then $u(x, y) = \sum_{n \in \mathbb{N}} u_n(x)\, \varphi_n(y)$, and

$$\begin{cases} u_n'' + k_n^2 u_n = f_n, \\ u_n \text{ is outgoing,} \end{cases} \qquad \text{with} \qquad k_n = \sqrt{k^2 - \frac{n^2\pi^2}{h^2}}. \tag{3}$$

Modal decomposition

We define each mode $n \in \mathbb{N}$ of the waveguide by

$$\varphi_n = \begin{cases} \dfrac{1}{\sqrt{h}} & \text{if } n = 0, \\ y \mapsto \dfrac{\sqrt{2}}{\sqrt{h}} \cos\left(\dfrac{n\pi y}{h}\right) & \text{else.} \end{cases} \tag{2}$$

Then $u(x,y) = \sum_{n\in\mathbb{N}} u_n(x)\,\varphi_n(y)$, and

$$\begin{cases} u_n'' + k_n^2 u_n = f_n, \\ u_n \text{ is outgoing,} \end{cases} \quad \text{with} \quad k_n = \sqrt{k^2 - \frac{n^2\pi^2}{h^2}}. \tag{3}$$

$$\Rightarrow \quad u_n(x) = \int_{\mathbb{R}} G_n(x,s) f_n(s)\mathrm{d}s, \quad G_n(x,s) = \frac{i}{2k_n}\varphi_n(1)e^{ik_n|x-s|}.$$

Modal decomposition

We define each mode $n \in \mathbb{N}$ of the waveguide by

$$\varphi_n = \begin{cases} \dfrac{1}{\sqrt{h}} & \text{if } n = 0, \\ y \mapsto \dfrac{\sqrt{2}}{\sqrt{h}} \cos\left(\dfrac{n\pi y}{h}\right) & \text{else.} \end{cases} \tag{2}$$

Then $u(x, y) = \sum_{n\in\mathbb{N}} u_n(x)\,\varphi_n(y)$, and

$$\begin{cases} u_n'' + k_n^2 u_n = f_n, \\ u_n \text{ is outgoing,} \end{cases} \quad \text{with} \quad k_n = \sqrt{k^2 - \frac{n^2\pi^2}{h^2}}. \tag{3}$$

$$\Rightarrow \quad u_n(x) = \int_{\mathbb{R}} G_n(x, s) f_n(s)\mathrm{d}s, \quad G_n(x, s) = \frac{i}{2k_n}\varphi_n(1)e^{ik_n|x-s|}.$$

Modal decomposition

We define each mode $n \in \mathbb{N}$ of the waveguide by

$$\varphi_n = \begin{cases} \dfrac{1}{\sqrt{h}} & \text{if } n = 0, \\ y \mapsto \dfrac{\sqrt{2}}{\sqrt{h}} \cos\left(\dfrac{n\pi y}{h}\right) & \text{else.} \end{cases} \tag{2}$$

Then $u(x,y) = \sum_{n\in\mathbb{N}} u_n(x)\,\varphi_n(y)$, and

$$\begin{cases} u_n'' + k_n^2 u_n = f_n, \\ u_n \text{ is outgoing,} \end{cases} \quad \text{with} \quad k_n = \sqrt{k^2 - \frac{n^2\pi^2}{h^2}}. \tag{3}$$

$$\Rightarrow \quad u_n(x) = \int_{\mathbb{R}} G_n(x,s) f_n(s)\mathrm{d}s, \quad G_n(x,s) = \frac{i}{2k_n}\varphi_n(1)e^{ik_n|x-s|}.$$

- If $n < kh/\pi$, the mode n is called propagative.
- If $n > kh/\pi$, the mode n is called evanescent.

Reconstruction de h

We measure $\|u\|_{L^2_{loc}}$ for all $k > 0$:

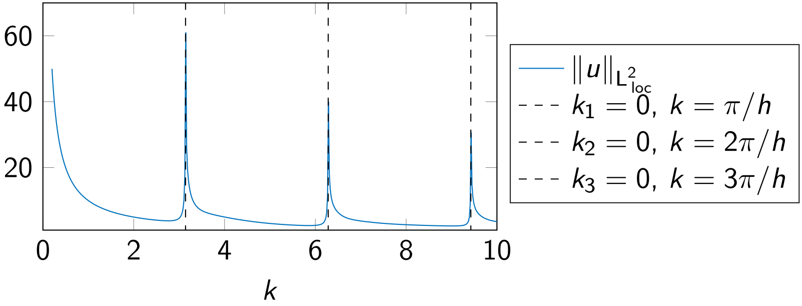

Figure: Amplitude of u with respect to k. We identify h by looking at explosions of $\|u\|_{L^2_{loc}}$.

$$\|u\| \to +\infty \quad \Leftrightarrow \quad k_n = 0 \quad \Leftrightarrow \quad k = \frac{n\pi}{h}. \tag{4}$$

Experimental setup at Institut Langevin

Expectations and ideas before the experimentations:

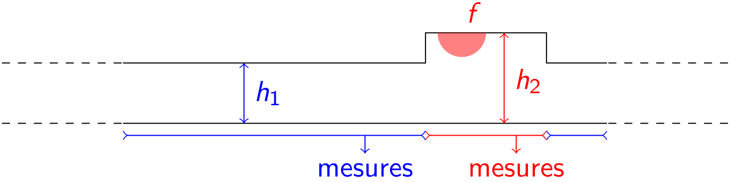

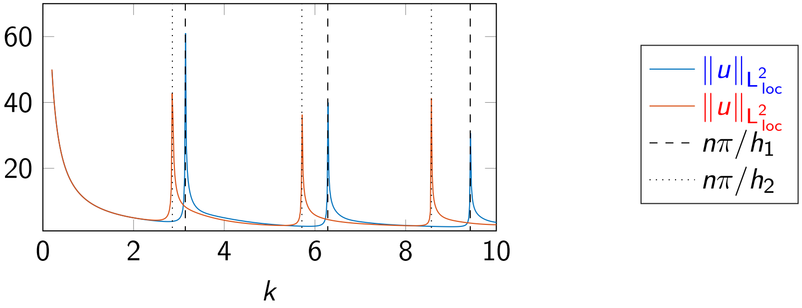

Experimental setup at Institut Langevin

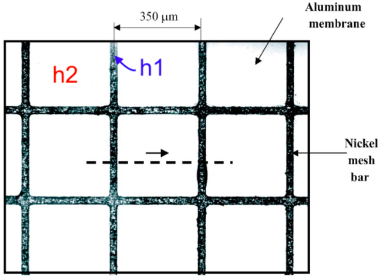

Figure: [Balogun 07] Left: 3D plate with two different widths. Right: amplitude of waves along the dotted line for different frequencies.

Experimental setup at Institut Langevin

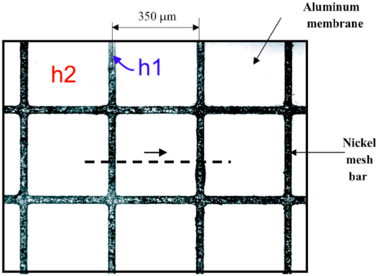

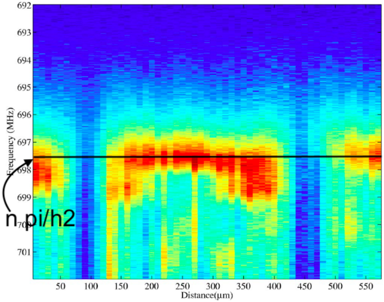

Figure: [BALOGUN 07] Left: 3D plate with two different widths. Right: amplitude of waves along the dotted line for different frequencies.

Experimental setup at Institut Langevin

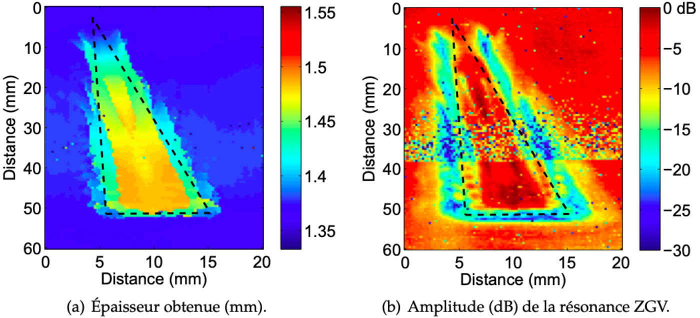

Figure: [Ces 12] Left: Experimental reconstruction of a width defect. Right: amplitude of explosions near resonances.

Modeling of the problem

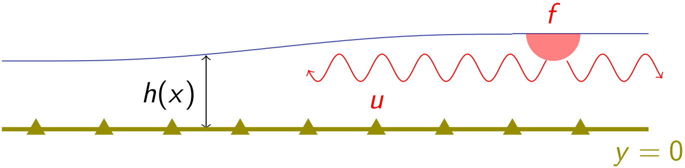

Figure: Parametrization of a slowly increasing waveguide. A source f generates a wavefield u measured on the bottom of the waveguide.

Modeling of the problem

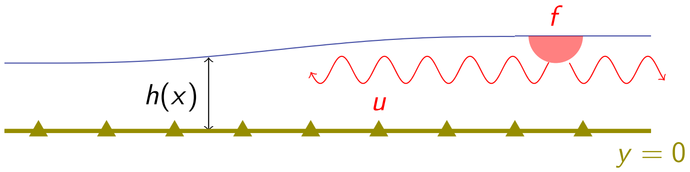

Figure: Parametrization of a slowly increasing waveguide. A source f generates a wavefield u measured on the bottom of the waveguide.

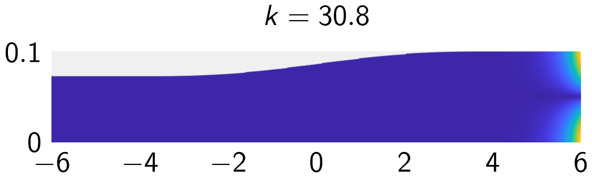

Figure: Numerical simulation of the amplitude of $|u|$ for different frequencies k.

Modeling of the problem

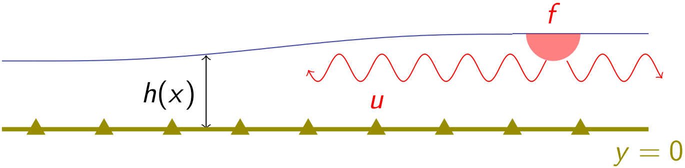

Figure: Parametrization of a slowly increasing waveguide. A source f generates a wavefield u measured on the bottom of the waveguide.

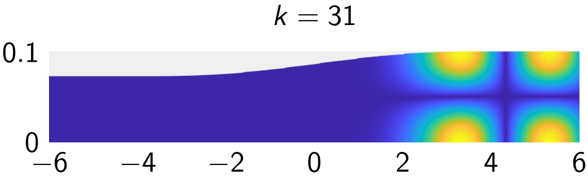

Figure: Numerical simulation of the amplitude of $|u|$ for different frequencies k.

Modeling of the problem

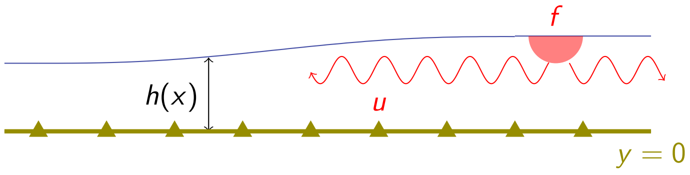

Figure: Parametrization of a slowly increasing waveguide. A source f generates a wavefield u measured on the bottom of the waveguide.

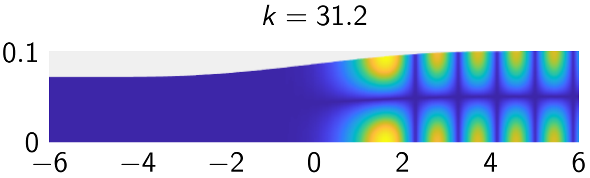

Figure: Numerical simulation of the amplitude of $|u|$ for different frequencies k.

Modeling of the problem

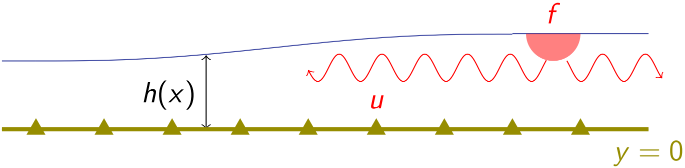

Figure: Parametrization of a slowly increasing waveguide. A source f generates a wavefield u measured on the bottom of the waveguide.

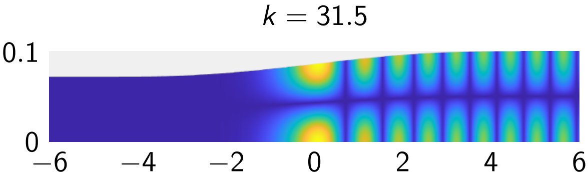

Figure: Numerical simulation of the amplitude of $|u|$ for different frequencies k.

Modeling of the problem

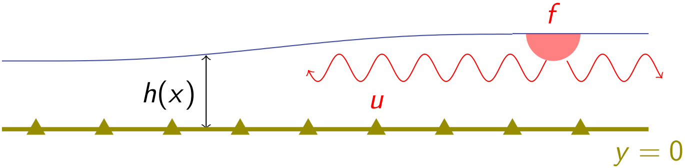

Figure: Parametrization of a slowly increasing waveguide. A source f generates a wavefield u measured on the bottom of the waveguide.

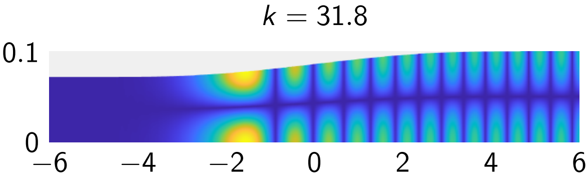

Figure: Numerical simulation of the amplitude of $|u|$ for different frequencies k.

Modeling of the problem

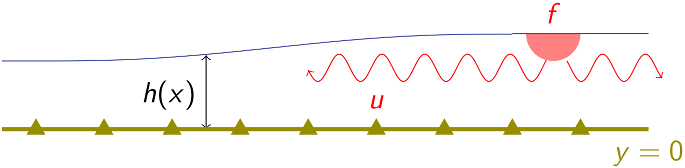

Figure: Parametrization of a slowly increasing waveguide. A source f generates a wavefield u measured on the bottom of the waveguide.

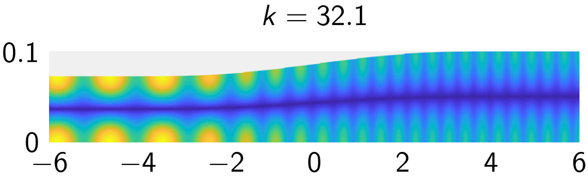

Figure: Numerical simulation of the amplitude of $|u|$ for different frequencies k.

Outline

Change of variable

In the perturbed waveguide Ω, the wavefield satisfies the equation

$$\begin{cases} \Delta u + k^2 u = -f & \text{in } \Omega, \\ \partial_\nu u = 0 & \text{on } \partial\Omega, \\ u \text{ is outgoing.} \end{cases} \tag{5}$$

Change of variable

In the perturbed waveguide Ω, the wavefield satisfies the equation

$$\begin{cases} \Delta u + k^2 u = -f & \text{in } \Omega, \\ \partial_\nu u = 0 & \text{on } \partial\Omega, \\ u \text{ is outgoing.} & \end{cases} \tag{5}$$

We define the mapping $\psi(x, y) = (x, h(x)y)$ from the perfect waveguide $\Omega^D = \mathbb{R} \times (0, 1)$ to Ω:

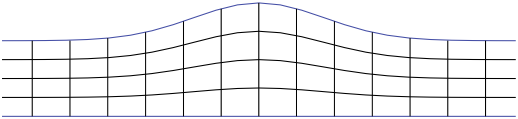

Figure: Mapping from Ω^D to Ω.

Change of variable

In the perturbed waveguide Ω, the wavefield satisfies the equation

$$\begin{cases} \Delta u + k^2 u = -f & \text{in } \Omega, \\ \partial_\nu u = 0 & \text{on } \partial\Omega, \\ u \text{ is outgoing.} \end{cases} \tag{5}$$

We define $\psi(x, y) = (x, h(x)y)$, and in the perfect waveguide $\Omega^D = \mathbb{R} \times (0, 1)$, $v = u \circ \psi$ satisfies

$$\begin{cases} \partial_{xx} v + k^2 v + \frac{1}{h^2}\partial_{yy} v - \frac{h''h - 2(h')^2}{h^3} y\partial_y v & \\ \quad + \frac{(h')^2}{h^4} y^2 \partial_{yy} v - \frac{2h'}{h^2} y \partial_{yx} v = -f \circ \psi & \text{in } \Omega^D, \\ \partial_\nu v = \frac{h'}{h}\partial_x v \mathbf{1}_{y=h(x)} & \text{on } \partial\Omega^D, \\ v \text{ is outgoing.} \end{cases} \tag{6}$$

We denote w the solution of the equation without the green terms.

Approximation of the solution

We use the modal decomposition of w and

$$\forall n \in \mathbb{N} \qquad w_n''(x) + k_n(x)^2 w_n(x) = -g_n(x) \quad \text{in } \mathbb{R}. \qquad (7)$$

We recognize a Schrödinger equation [Olver 61] [Olver 63].

Approximation of the solution

We use the modal decomposition of w and

$$\forall n \in \mathbb{N} \qquad w_n''(x) + k_n(x)^2 w_n(x) = -g_n(x) \quad \text{in } \mathbb{R}. \tag{7}$$

We recognize a Schrödinger equation [Olver 61] [Olver 63].

- If $k_n(x)^2 > 0$ for all $x \in \mathbb{R}$, the Green function is given by

$$G_n^{\text{app}}(x,s) := C_n(s) \exp\left(i \left| \int_s^x k_n \right| \right). \qquad \text{(propagative)}$$

Approximation of the solution

We use the modal decomposition of w and

$$\forall n \in \mathbb{N} \qquad w_n''(x) + k_n(x)^2 w_n(x) = -g_n(x) \quad \text{in } \mathbb{R}. \tag{7}$$

We recognize a Schrödinger equation [Olver 61] [Olver 63].

- If $k_n(x)^2 > 0$ for all $x \in \mathbb{R}$, the Green function is given by

$$G_n^{\mathrm{app}}(x,s) := C_n(s) \exp\left(i \left| \int_s^x k_n \right| \right). \qquad \text{(propagative)}$$

- If $k_n(x)^2 < 0$ for all $x \in \mathbb{R}$, the Green function is given by

$$G_n^{\mathrm{app}}(x,s) := C_n(s) \exp\left(- \left| \int_s^x k_n \right| \right). \qquad \text{(evanescent)}$$

Approximation of the solution

We use the modal decomposition of w and

$$\forall n \in \mathbb{N} \qquad w_n''(x) + k_n(x)^2 w_n(x) = -g_n(x) \quad \text{in } \mathbb{R}. \qquad (7)$$

We recognize a Schrödinger equation [Olver 61] [Olver 63].

- If $k_n(x)^2 > 0$ for all $x \in \mathbb{R}$, the Green function is given by

$$G_n^{\text{app}}(x,s) := C_n(s) \exp\left(i \left| \int_s^x k_n \right| \right). \qquad \text{(propagative)}$$

- If $k_n(x)^2 < 0$ for all $x \in \mathbb{R}$, the Green function is given by

$$G_n^{\text{app}}(x,s) := C_n(s) \exp\left(- \left| \int_s^x k_n \right| \right). \qquad \text{(evanescent)}$$

- If there exists a point $x^\star$ such that $k_n(x^\star) = 0$,

$$G_n^{\text{app}}(x,s) := C_n(s)\, \mathcal{A}\left(- \left(\frac{3}{2} \int_{x^\star}^x k_n \right)^{2/3} \right), \quad \text{(loc. resonant)}$$

where $\mathcal{A}$ is the first kind Airy function and $x^\star < x < s$.

Forward problem

Theorem - Approximation of u in slowly varying waveguides

[Bonnetier, Niclas, Seppecher, Vial 22]

Let $r > 0$, $f \in \mathrm{L}^2(\Omega_r)$, $h \in \mathcal{C}^2(\mathbb{R})$ with h' compactly supported. For almost every frequencies $k > 0$, if $\|h'\|_{\mathrm{W}^{1,1}(\mathbb{R})}$ is small enough then

- The Helmholtz problem in the perturbed waveguide has a unique solution $u \in \mathrm{H}^2_{\mathrm{loc}}(\Omega)$.
- This solution can be approximated by

$$u^{app}(x,y) = \sum_{n\in\mathbb{N}} \left(\int_{\mathbb{R}} G_n^{app}(x,s) g_n(s) \mathrm{d}s \right) \varphi_n \left(\frac{y}{h(x)} \right). \quad (8)$$

- There exists a constant $C > 0$ such that

$$\|u - u^{app}\|_{\mathrm{H}^1(\Omega_r)} \leq C \|h'\|_{\mathrm{W}^{1,1}(\mathbb{R})} \|f\|_{\mathrm{L}^2(\Omega_r)}. \quad (9)$$

Numerical illustration

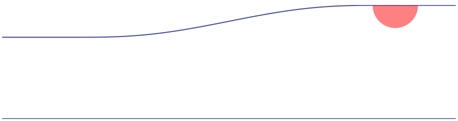

Figure: Wavefield approximation of $\mathrm{Re}(u)$ in a slowly varying waveguide at the frequency $k = 31.5$ using the modal decomposition of u^{app} and each G_n^{app}.

Numerical illustration

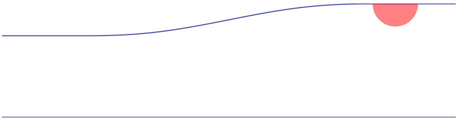

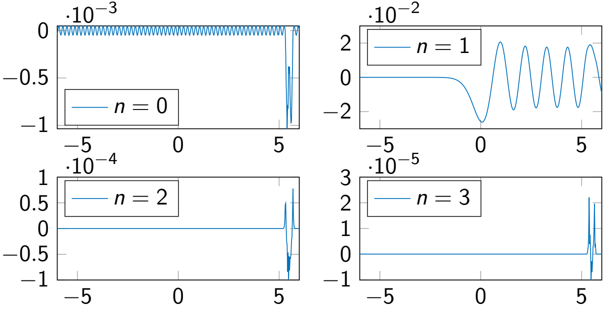

Figure: Wavefield approximation of $\mathrm{Re}(u)$ in a slowly varying waveguide at the frequency $k = 31.5$ using the modal decomposition of u^{app} and each G_n^{app}.

Numerical illustration

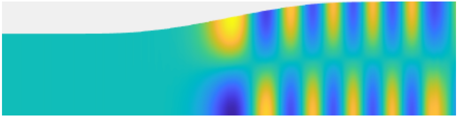

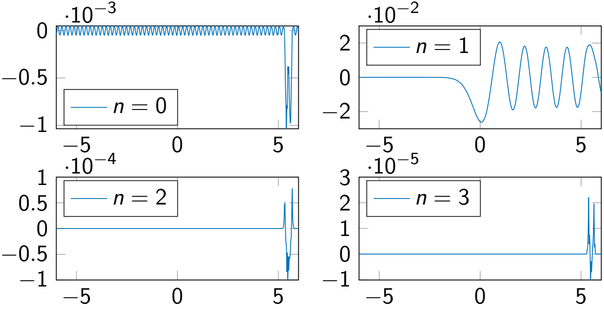

Figure: Wavefield approximation of $\mathrm{Re}(u)$ in a slowly varying waveguide at the frequency $k = 31.5$ using the modal decomposition of u^{app} and each G_n^{app}.

Tunneling effect

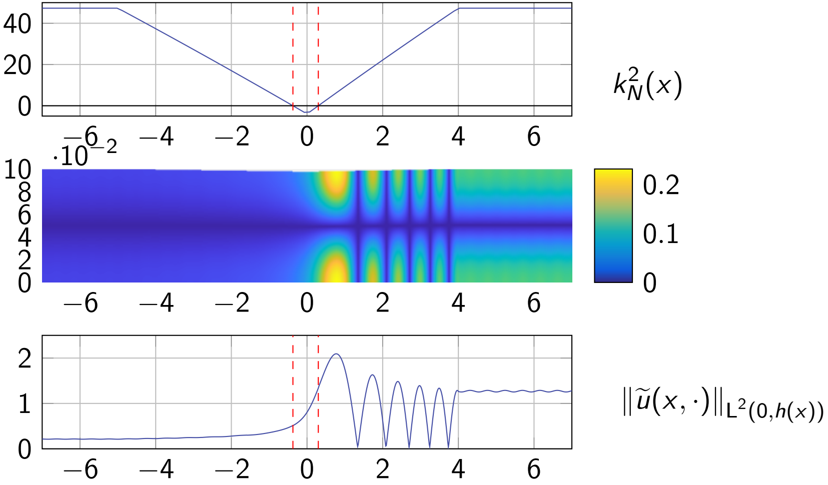

Figure: Illustration of a tunneling effect in a perturbed waveguide.

Locally resonant point $x^\star$

$k = 31.2$

$k = 31.5$

$k = 31.8$

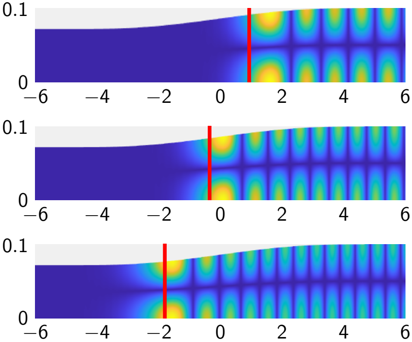

Figure: Wavefield $|u|$ for different locally resonant frequencies k. The position $x = x^\star$ is marked in red.

Locally resonant point $x^\star$

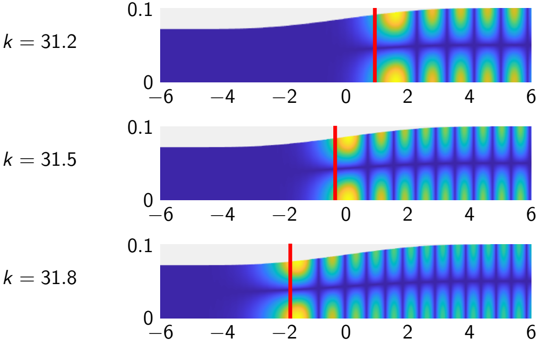

Figure: Wavefield $|u|$ for different locally resonant frequencies k. The position $x = x^\star$ is marked in red.

If we recover the position of $x^\star$, we know the local width

$$k_n(x^\star) = 0 \quad \Leftrightarrow \quad h(x^\star) = \frac{n\pi}{k}. \tag{10}$$

Filtering of measurements

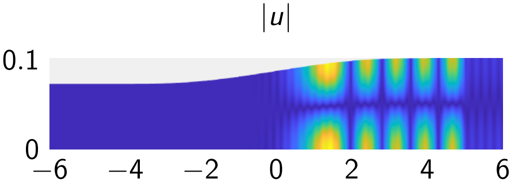

Figure: Measurements and filtering of the data for a locally resonant mode.

Filtering of measurements

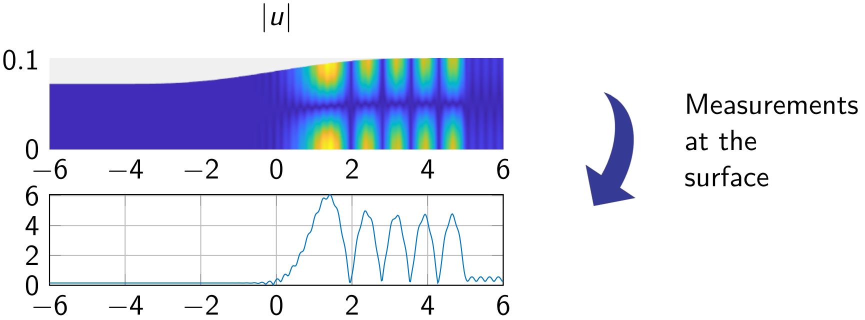

Figure: Measurements and filtering of the data for a locally resonant mode.

Filtering of measurements

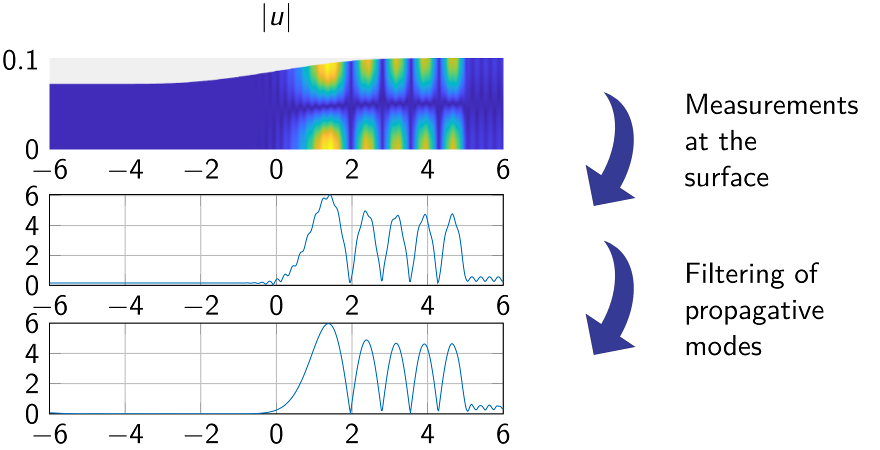

Figure: Measurements and filtering of the data for a locally resonant mode.

Reconstruction of $x^\star$

Doing a Taylor expansion on G_n^{app}, we notice that around $x^\star$, the data d satisfy

$$d \approx f_N * \left[C_N \mathcal{A}\left(-\left(\frac{3}{2} \int_{x^\star}^{x} k_N \right)^{2/3} \right) \right] \approx z\mathcal{A}(\alpha(x - x^\star)), \quad (11)$$

where $z, \alpha > 0$. We minimize the function

$$J(z, \alpha, x^\star) = \|z\mathcal{A}(\alpha(x - x^\star)) - d\|_2^2. \quad (12)$$

Reconstruction of $x^\star$

Doing a Taylor expansion on G_n^{app}, we notice that around $x^\star$, the data d satisfy

$$d \approx f_N * \left[C_N \mathcal{A}\left(-\left(\frac{3}{2} \int_{x^\star}^{x} k_N \right)^{2/3} \right) \right] \approx z\mathcal{A}(\alpha(x - x^\star)), \qquad (11)$$

where $z, \alpha > 0$. We minimize the function

$$J(z, \alpha, x^\star) = \|z\mathcal{A}(\alpha(x - x^\star)) - d\|_2^2. \qquad (12)$$

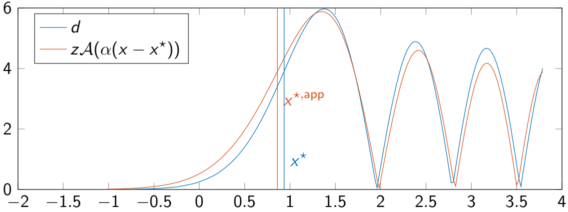

Figure: Comparison between the data d and the Airy function obtained by minimizing J.

Stability of the reconstruction

Theorem - stability of the reconstruction of $x^\star$
[Niclas, Seppecher 22]

We denote $d = |u(x,0)| + \varepsilon(x)$ for $x \in I := (x^\star - R, x^\star + R)$. If $\|\varepsilon\|_{\mathrm{L}^2(I)}$ and $\|h'\|_{\mathrm{W}^{1,1}(\mathbb{R})}$ are small enough, then

- The function J has a unique minimum denoted $(z^{\mathrm{app}}, \alpha^{\mathrm{app}}, x^{\star,\mathrm{app}})$.
- There exist constants $C_1, C_2 > 0$ such that

$$|x^\star - x^{\star,\mathrm{app}}| \leq C_1 \|h'\|^{1/3}_{\mathrm{W}^{1,1}(\mathbb{R})} + C_2 \|\varepsilon\|_{\mathrm{L}^2(I)}. \tag{13}$$

- There exists a neighborhood $V \subset \mathbb{R}^3$ such that a gradient descent starting in V converges to $(z^{\mathrm{app}}, \alpha^{\mathrm{app}}, x^{\star,\mathrm{app}})$.

Numerical results

For different locally resonant frequencies $k > 0$, we reconstruct $x^\star$ and then $h(x^\star)$.

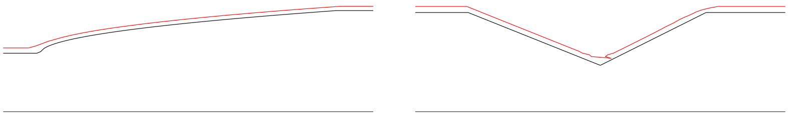

Figure: Reconstruction of slowly varying varying defects. Black: initial shape. Red: reconstruction slightly shifted.

Numerical results

For different locally resonant frequencies $k > 0$, we reconstruct $x^\star$ and then $h(x^\star)$.

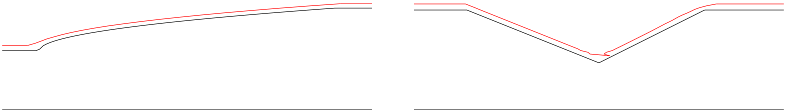

Figure: Reconstruction of slowly varying varying defects. Black: initial shape. Red: reconstruction slightly shifted.

$\|h'\|_{W^{1,\infty}}$	0.05	5
k non résonant	5%	54%

$\|\varepsilon\|_{L^2(I)}$	1%	15%
k non résonant	6.2%	45%

Figure: Relative reconstruction errors.

Numerical results

For different locally resonant frequencies $k > 0$, we reconstruct $x^\star$ and then $h(x^\star)$.

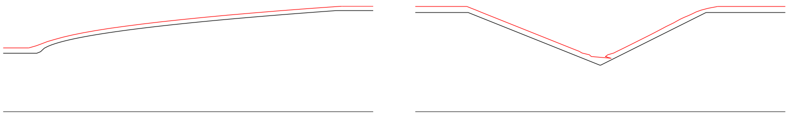

Figure: Reconstruction of slowly varying varying defects. Black: initial shape. Red: reconstruction slightly shifted.

$\|h'\|_{W^{1,\infty}}$	0.05	5
k non résonant	5%	54%
k résonant	1%	9%

$\|\varepsilon\|_{L^2(I)}$	1%	15%
k non résonant	6.2%	45%
k résonant	1.3%	7%

Figure: Relative reconstruction errors.

Outline

Modal decomposition using Lamb modes

A source $\boldsymbol{f}$ generates an elastic displacement field $\boldsymbol{u}$ satisfying

$$\begin{cases} \nabla \cdot \boldsymbol{\sigma}(\boldsymbol{u}) + \omega^2 \boldsymbol{u} = -\boldsymbol{f} & \text{in } \Omega, \\ \boldsymbol{\sigma}(\boldsymbol{u}) \cdot \nu = 0 & \text{on } \partial\Omega, \end{cases} \tag{14}$$

where $\boldsymbol{\sigma}$ the stress tensor depending on the Lamé parameters of the waveguide, ω the frequency.

Modal decomposition at width h for almost every $\omega \in \mathbb{R}_+$:

$$\boldsymbol{u}(x, y) = \sum_{n>0} (a_n(x) u_n(y), b_n(x) v_n(y)), \tag{15}$$

Modal decomposition using Lamb modes

A source $\boldsymbol{f}$ generates an elastic displacement field $\boldsymbol{u}$ satisfying

$$\begin{cases} \nabla \cdot \boldsymbol{\sigma}(\boldsymbol{u}) + \omega^2 \boldsymbol{u} = -\boldsymbol{f} & \text{in } \Omega, \\ \boldsymbol{\sigma}(\boldsymbol{u}) \cdot \nu = 0 & \text{on } \partial\Omega, \end{cases} \tag{14}$$

where $\boldsymbol{\sigma}$ the stress tensor depending on the Lamé parameters of the waveguide, ω the frequency.

Modal decomposition at width h for almost every $\omega \in \mathbb{R}_+$:

$$\boldsymbol{u}(x, y) = \sum_{n>0} (a_n(x) u_n(y), b_n(x) v_n(y)), \tag{15}$$

(u_n, v_n) are Lamb modes associated to the wavenumber $k_n \in \mathbb{C}$.

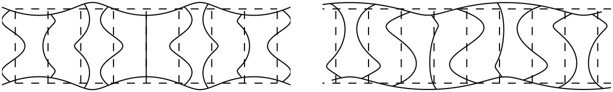

Figure: Elastic deformation of a plate $e^{ik_n x}(u_n(y), v_n(y))$ for a symmetric and an anti-symmetric Lamb mode.

Adaptation of locally resonant frequencies

Main steps of the inversion using locally resonant frequencies

- Choose a locally resonant frequency
- Approximate the wavefield generated by a known source term in the waveguide
- Fit the three-parameter Airy function to the measurements to recover the location of $x^\star$
- Reconstruct the width of the waveguide using the knowledge of $x^\star$ and $h(x^\star)$ for different locally resonant frequencies

Adaptation of locally resonant frequencies

Main steps of the inversion using locally resonant frequencies

- Choose a locally resonant frequency
- Approximate the wavefield generated by a known source term in the waveguide
- Fit the three-parameter Airy function to the measurements to recover the location of $x^\star$
- Reconstruct the width of the waveguide using the knowledge of $x^\star$ and $h(x^\star)$ for different locally resonant frequencies

Resonant frequencies

Acoustic case: $k_n = \sqrt{k^2 - n^2\pi^2/h^2}$

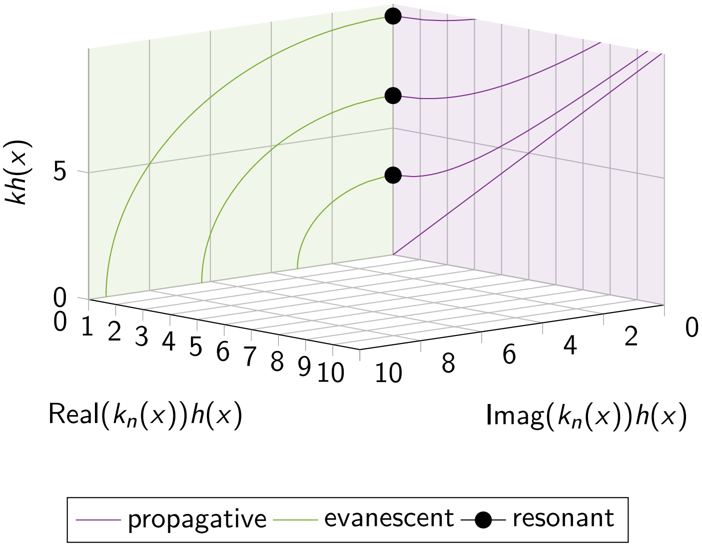

Resonant frequencies

Elastic case: $\mathcal{R}(\omega, h, k_n) = 0$

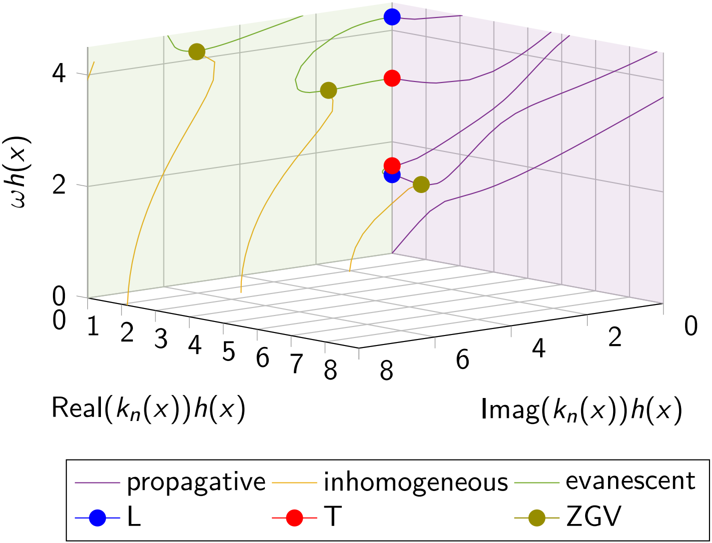

Modified Lamb basis

Proposition [Akian 22] [Bonnetier, Niclas, Seppecher 22]

Lamb modes associated to the frequency ω at width h form a complete family if and only if ωh is not a resonant point.

Modified Lamb basis

Proposition [Akian 22] [Bonnetier, Niclas, Seppecher 22]

Lamb modes associated to the frequency ω at width h form a complete family if and only if ωh is not a resonant point.

- Longitudinal point (L): $k_n = 0$, $u_n = 0$. New Lamb basis from [Pagneux, Maurel 06]

$$\widetilde{u_n} = \frac{u_n}{\langle u_n, v_n \rangle}, \qquad \widetilde{v_n} = v_n.$$

- Transverse point (T): $k_n = 0$, $v_n/k_n = 0$. New Lamb basis from [Pagneux, Maurel 06]

$$\widetilde{u_n} = \frac{u_n}{k_n}, \qquad \widetilde{v_n} = \frac{k_n v_n}{\langle u_n, v_n \rangle}.$$

- Zero-group velocity point (ZGV): $k_n \neq 0$. New Lamb basis

$$\widetilde{u_1} = \frac{u_1 - u_2}{2}, \quad \widetilde{v_1} = \frac{v_1 + v_2}{2}, \quad \widetilde{u_2} = \frac{u_1 + u_2}{2\langle u_1, v_1 \rangle}, \quad \widetilde{v_2} = \frac{v_1 - v_2}{2\langle u_1, v_1 \rangle}.$$

Approximation of the wavefield

Modal decomposition of the wavefield:

$$\boldsymbol{u}(x,y) = \sum_{n\geq 1} \left(a_n(x)\widetilde{u_n}(x,y), b_n(x)\widetilde{v_n}(x,y)\right). \tag{16}$$

Approximation of the wavefield

Modal decomposition of the wavefield:

$$\boldsymbol{u}(x,y) = \sum_{n\geq 1} \left(a_n(x)\widetilde{u_n}(x,y), b_n(x)\widetilde{v_n}(x,y)\right). \tag{16}$$

- Longitudinal point (L): $b_N \approx G_N^{\text{app}} * F_N$, and

$$\boldsymbol{u}_1 \approx z\mathcal{A}(\alpha(x - x^\star)). \tag{17}$$

- Transverse point (T): $a_N \approx G_N^{\text{app}} * F_N$, and

$$\boldsymbol{u}_2 \approx z\mathcal{A}(\alpha(x - x^\star)). \tag{18}$$

- Zero-group velocity point (ZGV):

$$\left|\frac{\boldsymbol{u}_1}{c_1} + \frac{\boldsymbol{u}_2}{c_2}\right| \approx z|\mathcal{A}(\alpha(x - x^\star))|. \tag{19}$$

Reconstruction of h

Figure: Reconstruction of two width profiles. Black: initial shape. Red: reconstruction slightly shifted for comparison purposes.

$\|h'\|_{W^{1,\infty}}$	9.10^{-4}	3.10^{-3}	7.10^{-3}	1.10^{-2}
L, $\|h - h^{app}\|_\infty / \|h\|_\infty$	2.8%	7.6%	13.2%	23.4%
T, $\|h - h^{app}\|_\infty / \|h\|_\infty$	2.9%	5.3%	10.2%	17.4%
ZGV, $\|h - h^{app}\|_\infty / \|h\|_\infty$	1.7%	2.3%	5.7%	8.2%

Table: Relative errors on the reconstruction for increasing values of $\|h'\|$

Outline

Piecewise constant widths

Aim: Generalize the use of locally resonances for any variation of the width. We are especially interested in piecewise constant widths.

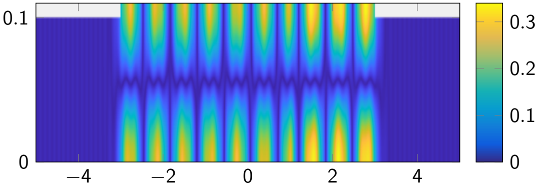

Figure: Numerical simulation of the wavefield propagation in a waveguide with width steps.

➤ Ongoing collaboration with Institut Langevin (Claire Prada, Daniel Kieffer, François Legrand).

3D acoustic waveguides

Aim: Extend the method to the 3D acoustic case to recover complex width defects.

- We should be able to recover a part of the spectrum $(\lambda_n(x))_{n=1,\cdots,N})$ for each section
- We need to find a link between these data and the width h

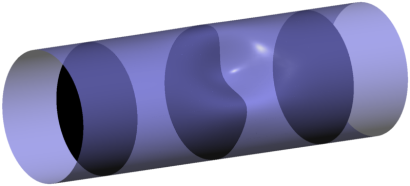

Figure: Sections of a perturbed 3D acoustic waveguide

➤ Ongoing collaboration with Saint Gobain Research Paris (Marion Perrodin).

Torsional waves in thin elastic cylinders

Aim: Reconstruct inhomogeneities and width defects in thin elastic cylinders. We expect to do this using thin layers approximations.

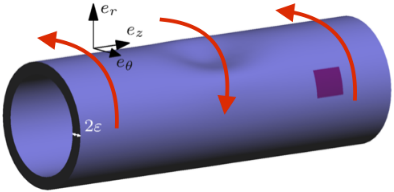

Figure: Modeling of a thin elastic cylinder where torsional waves are propagating.

➤ Work in progress with Eric Soccorsi (Aix Marseille University). Ongoing collaboration with LTDS (Olivier Bareille, Mohamed Kharrat).

Passive imaging of a randomly perturbed medium

Aim: Better understand how to reconstruct certain parameters of the Earth's layer using tails of seismographs.

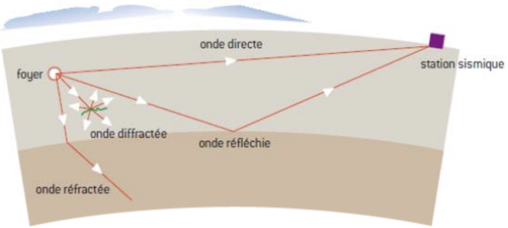

Figure: Modeling of the first Earth's layer as a waveguide.

➤ Work in progress with Josselin Garnier (Ecole Polytechnique).

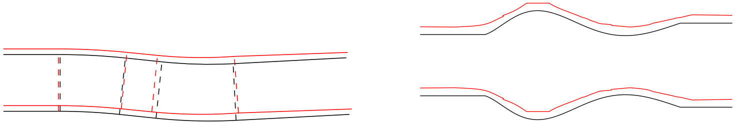

Thank you for your attention!